

Evolutionary Optimization of Deep Learning Activation Functions*

Garrett Bingham

The University of Texas at Austin and
Cognizant Technology Solutions
San Francisco, California
bingham@cs.utexas.edu

William Macke

The University of Texas at Austin
Austin, Texas
wmacke@cs.utexas.edu

Risto Miikkulainen

The University of Texas at Austin and
Cognizant Technology Solutions
San Francisco, California
risto@cs.utexas.edu

ABSTRACT

The choice of activation function can have a large effect on the performance of a neural network. While there have been some attempts to hand-engineer novel activation functions, the Rectified Linear Unit (ReLU) remains the most commonly-used in practice. This paper shows that evolutionary algorithms can discover novel activation functions that outperform ReLU. A tree-based search space of candidate activation functions is defined and explored with mutation, crossover, and exhaustive search. Experiments on training wide residual networks on the CIFAR-10 and CIFAR-100 image datasets show that this approach is effective. Replacing ReLU with evolved activation functions results in statistically significant increases in network accuracy. Optimal performance is achieved when evolution is allowed to customize activation functions to a particular task; however, these novel activation functions are shown to generalize, achieving high performance across tasks. Evolutionary optimization of activation functions is therefore a promising new dimension of metalearning in neural networks.

CCS CONCEPTS

• **Computing methodologies** → **Neural networks**; Object identification; • **Theory of computation** → *Evolutionary algorithms*;

KEYWORDS

Activation functions, evolutionary algorithms, metalearning

ACM Reference Format:

Garrett Bingham, William Macke, and Risto Miikkulainen. 2020. Evolutionary Optimization of Deep Learning Activation Functions. In *Genetic and Evolutionary Computation Conference (GECCO '20)*, July 8–12, 2020, Cancún, Mexico. ACM, New York, NY, USA, 8 pages. <https://doi.org/10.1145/3377930.3389841>

1 INTRODUCTION

Together with topology, loss function, and learning rate, the choice of activation function plays a large role in determining how a

neural network learns and behaves. An activation can be any arbitrary function that transforms the output of a layer in a neural network. However, only a small number of activation functions are widely used in modern deep learning architectures. The Rectified Linear Unit, $\text{ReLU}(x) = \max\{x, 0\}$, is popular because it is simple and effective. Other activation functions such as $\tanh(x)$ and $\sigma(x) = 1/(1 + e^{-x})$ are commonly used when it is useful to restrict the activation value within a certain range. There have also been attempts to engineer new activation functions to have certain properties. For example, Leaky ReLU [11] allows information to flow when $x < 0$. Softplus [13] is positive, monotonic, and smooth. Many hand-engineered activation functions exist [15], but none have achieved widespread adoption comparable to ReLU. Activation function design can therefore be seen as a largely untapped resource in neural network design.

This situation points to an interesting opportunity: it may be possible to optimize activation functions automatically through metalearning. Rather than attempting to directly optimize a single model as in traditional machine learning, metalearning seeks to find better performance over a space of models, such as a collection of network architectures, hyperparameters, learning rates, or loss functions [4–8, 20]. Several techniques for metalearning have been proposed, including gradient descent, Bayesian hyperparameter optimization, reinforcement learning, and evolutionary algorithms [3, 5, 17, 23]. Of these, evolution is the most versatile and can be applied to several aspects of neural network design.

This work develops an evolutionary approach to optimize activation functions. Activation functions are represented as trees, and novel activation functions are discovered through crossover, mutation, and exhaustive search in expressive search spaces containing billions of candidate activation functions. The resulting functions are unlikely to be discovered manually, yet they perform well, surpassing traditional activation functions like ReLU on image classification tasks CIFAR-10 and CIFAR-100.

This paper continues with Section 2, which presents a summary of related research in metalearning and neural network optimization, and discusses how this work furthers the field. Section 3 explains how activation functions are evolved in detail, defining the search space of candidate functions as well as the implementation of crossover and mutation. In Section 4, a number of search strategies are presented, and results of the experiments are given in Section 5. This work continues with discussion and potential future work in Section 6, before concluding in Section 7.

*G. Bingham and W. Macke contributed equally.

Permission to make digital or hard copies of all or part of this work for personal or classroom use is granted without fee provided that copies are not made or distributed for profit or commercial advantage and that copies bear this notice and the full citation on the first page. Copyrights for components of this work owned by others than ACM must be honored. Abstracting with credit is permitted. To copy otherwise, or republish, to post on servers or to redistribute to lists, requires prior specific permission and/or a fee. Request permissions from permissions@acm.org.

GECCO '20, July 8–12, 2020, Cancún, Mexico

© 2020 Association for Computing Machinery.

ACM ISBN 978-1-4503-7128-5/20/07...\$15.00

<https://doi.org/10.1145/3377930.3389841>

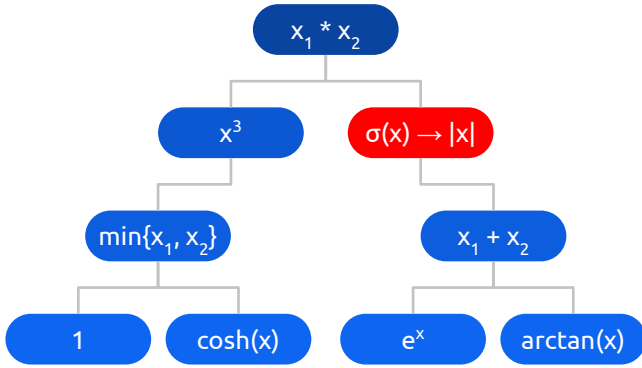


Figure 1: An example of activation function mutation. The tree represents the activation function $(\min\{1, \cosh(x)\})^3 * \sigma(e^x + \arctan(x))$. One node in the tree is selected uniformly at random and replaced with another operator in the search space, also uniformly at random. The resulting activation function is $(\min\{1, \cosh(x)\})^3 * |e^x + \arctan(x)|$. By introducing variability, mutation ensures evolution explores the search space sufficiently. It prevents high-performing activation functions from overly skewing the early generations of the search process.

2 RELATED WORK

There has been a significant amount of recent work on metalearning with neural networks. Neuroevolution, the optimization of neural network architectures with evolutionary algorithms, is one of the most popular approaches [4, 20]. Real et al. [18] proposed a scheme where pairs of architectures are sampled, mutated, and the better of the two is trained while the other is discarded. Xie and Yuille [21] implemented a full genetic algorithm with crossover to search for architectures. Real et al. [17] introduced a novel evolutionary approach called aging evolution to discover an architecture that achieved higher ImageNet classification accuracy than any previous human-designed architecture. Beyond neuroevolution, other approaches to neural architecture search include Monte Carlo tree search to explore a space of architectures [14] and reinforcement learning (RL) to automatically generate architectures through value function methods [2] and policy gradient approaches [23].

While the above work focuses on optimizing neural network topologies, some work has also focused on optimizing other aspects of neural networks. For instance, Gonzalez and Miikkulainen [8] used a genetic algorithm to construct novel loss functions, and then optimized the coefficients of the loss functions with a covariance-matrix adaptation evolutionary strategy. They discovered a loss function that results in faster training and higher accuracy compared to the standard cross-entropy loss. Marchisio et al. [12] introduced a method to automatically choose an activation function for each layer of a neural network, and Hagg et al. [9] augmented the NEAT algorithm [19] to simultaneously evolve per-neuron activation functions and the overall network topology. Another example is work by Ramachandran et al. [16], which automatically designed novel activation functions using RL.

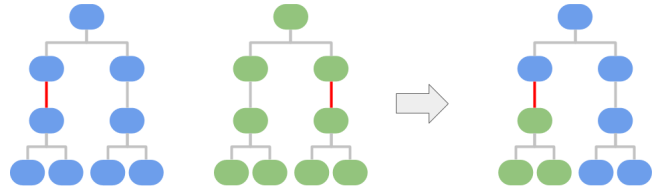


Figure 2: In crossover, two parent activation functions exchange randomly selected subtrees of equivalent depth, producing one new child activation function. Crossover enables the best activation functions to pass on their characteristics to the rest of the population. This mechanism is what enables evolution to discover better activation functions more quickly than random search.

This work expands upon previous research by introducing an evolutionary algorithm to design novel activation functions. While Marchisio et al. [12] and Hagg et al. [9] selected activation functions from predefined lists, this approach searches among billions of candidate activation functions. Although Ramachandran et al. [16] discovered a number of novel, high-performing activation functions with RL, they analyzed just one in depth: $x \cdot \sigma(x)$, which they call Swish. This paper takes activation function design a step further: instead of only searching for a single activation function that performs reasonably well for most datasets and neural network architectures, it demonstrates that it is possible to evolve specialized activation functions that perform particularly well for specific datasets and neural network architectures, thus utilizing the full power of metalearning.

3 EVOLVING ACTIVATION FUNCTIONS

This section presents the approach to evolving activation functions, introducing the search space, mutation and crossover implementations, and the overall evolutionary algorithm.

3.1 Search Space

Each activation function is represented as a tree consisting of unary and binary operators. Functions are grouped in layers such that two unary operators always feed into one binary operator. The following operators, modified slightly from the search space of Ramachandran et al. [16], are used:

- **Unary:** $0, 1, x, -x, |x|, x^2, x^3, \sqrt{x}, e^x, e^{-x^2}, \log(1 + e^x), \log(|x + \epsilon|), \sin(x), \sinh(x), \operatorname{arcsinh}(x), \cos(x), \cosh(x), \tanh(x), \operatorname{arctanh}(x), \max\{x, 0\}, \min\{x, 0\}, \sigma(x), \operatorname{erf}(x), \operatorname{sinc}(x)$
- **Binary:** $x_1 + x_2, x_1 - x_2, x_1 \cdot x_2, x_1 / (x_2 + \epsilon), \max\{x_1, x_2\}, \min\{x_1, x_2\}$

Following Ramachandran et al., a “core unit” is an activation function that can be represented as $\text{core_unit} = \text{binary}(\text{unary1}(x), \text{unary2}(x))$. Let F be the set of balanced core unit trees. S is then defined as a family of search spaces

$$S_{d \in \mathbb{N}} = \{f \in F \mid \text{depth}(f) = d\}. \quad (1)$$

For example, S_1 corresponds to the set of functions that can be represented by one core unit, S_2 represents functions of the form:

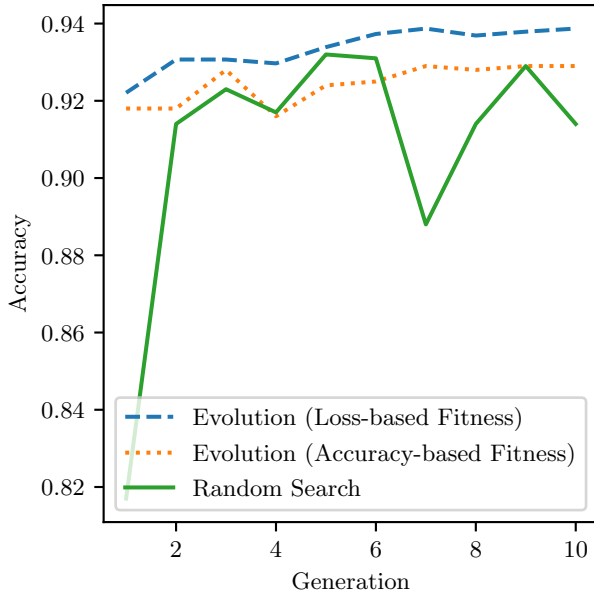


Figure 3: Top validation accuracy per generation for three search strategies in the S_2 search space. There are 50 activation functions in each generation of a search. All activation functions are trained with WRN-28-10 on CIFAR-10 for 50 epochs, and the highest validation accuracy obtained among all activation functions in a given generation is reported. Evolution with loss-based fitness finds better activation functions more quickly than evolution with accuracy-based fitness or random search. The first generation of random search is poor due to chance; since each generation is independent, the generations of random search could be arbitrarily reordered.

core_unit1(core_unit2(x), core_unit3(x)), and so on. Examples of functions in S_2 are illustrated in Figures 1 and 2.

3.2 Mutation

In mutation, one node in an activation function tree is selected uniformly at random. The operator at that node is replaced with another random operator in the search space. Unary operators are always replaced with unary operators, and binary operators with binary operators. An example of mutation is shown in Figure 1. Theoretically, mutation alone is sufficient for constructing any activation function. However, preliminary experiments showed that crossover can increase the rate at which good activation functions are found.

3.3 Crossover

In crossover, two parent activation functions exchange randomly selected subtrees, producing one new child activation function. The subtrees are constrained to be of the same depth, ensuring the child activation function is a member of the same search space as its parents. Crossover is depicted in Figure 2.

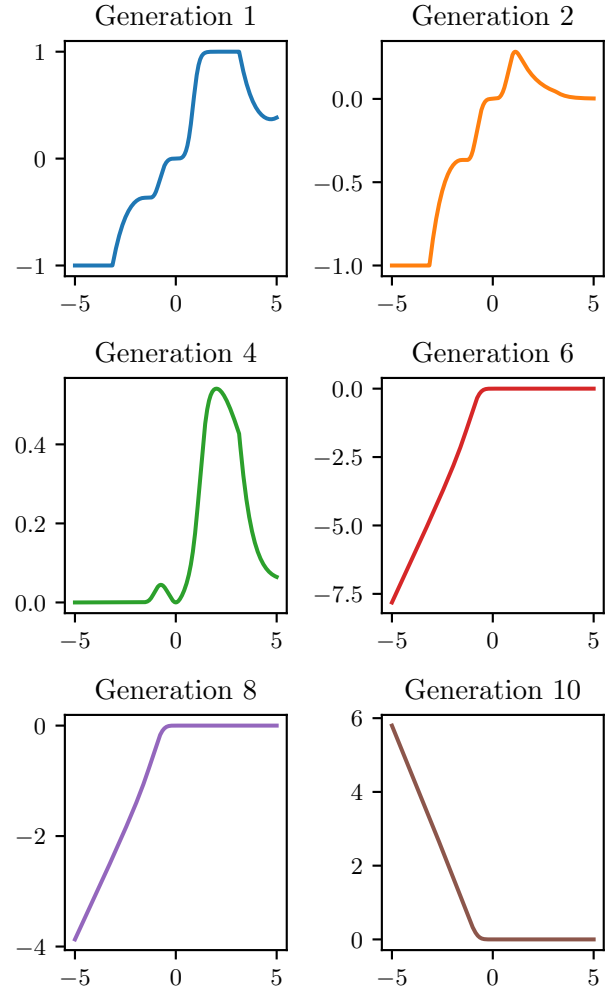


Figure 4: Best activation function by WRN-28-10 validation accuracy after 50 epochs of training on CIFAR-10 using evolution with loss-based fitness. Top validation accuracy improves from 92.2 in Generation 1 to 93.9 in Generation 10. Evolution is able to discover effective activation functions that are not likely to be discovered by hand. In particular, the top activation function discovered by evolution is smooth everywhere, unlike ReLU, which is not smooth at $x = 0$. This difference is likely the reason for its superior performance.

3.4 Evolution

Starting with a population of N activation functions, a neural network is trained with each function on a given training dataset. Each function is assigned a fitness p_i equal to the softmax of an evaluation metric L_j . This metric could be either accuracy or negative loss obtained on the validation dataset. More specifically,

$$p_i = \frac{e^{L_i}}{\sum_{j=1..N} e^{L_j}}. \quad (2)$$


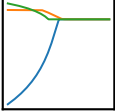
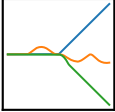
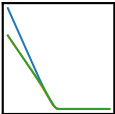
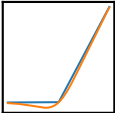
Function Plots		Accuracy	
		CIFAR-10	CIFAR-100
	Evolution with Loss-based Fitness (S_2)		
	• $(e^{\min\{\text{erf}(x), 0\}} - \max\{x, 0\}) * (\min\{\arctan((x)^3) * (\max\{ x , 0\}), 0\})$	94.1	73.9
	• $(e^{\max\{\min\{\text{erf}(x), 0\}, \max\{x, 0\}\}} * (\min\{\arctan((x)^3) * (\max\{ x , 0\}), 0\})$	10.0	01.0
	• $(-\arctan((x)^3) * (\cos(1))) * (-\arctan(\min\{x, 0\}) * (\max\{ x , 0\}))$	93.9	74.1
	Evolution with Accuracy-based Fitness (S_2)		
	• $\min\{e^{-\min\{(\sinh(x))^2, (0)^2\}}, \min\{\min\{\text{erf}(\log(1 + e^x)), \text{arcsinh}(x)\}, 0\}\}$	10.0	01.0
	• $\min\{\cos(\max\{\min\{x, 0\}^3, \log(1 + e^1)\}), e^{-\left(\max\{x, 0\} + e^{\sigma(x)}\right)^2}\}$	93.5	72.5
	• $\max\{\max\{(\log(\min\{x, 0\} + \epsilon)) * (\sigma(\text{erf}(x))), 0\}, 0\}$ (*)	92.5	72.3
	Random Search (S_2)		
	• $(\min\{\max\{(\log((x) + \epsilon))^3, -\log((x) + \epsilon)\}, 0\} + (e^{\min\{\tanh(x), 0\} + \log(\max\{x, 0\} + \epsilon)}) (*)$	93.8	73.9
	• $(\arctan(\min\{\sinh(\sin(x)), \arctan(\max\{x, 0\})\})) * (\tanh(-\sin(x)) * (\text{arcsinh}(x)))$	93.3	72.1
	• $(\max\{\frac{\min\{(x)^3, 0\}}{\max\{\sin(x), 0\} + \epsilon}, 0\}) - (\min\{(x)^2, \max\{x, 0\}\})$	93.9	73.2
	Exhaustive Search (S_1)		
	• $(\arctan(x)) * (\min\{x, 0\})$	94.0	74.5
	• $(\tanh(x)) * (\min\{x, 0\})$	94.1	74.3
	• $(\min\{x, 0\}) * (\text{erf}(x))$	94.0	74.2
	Baseline Activation Functions		
	• ReLU(x)	94.0	73.3
	• Swish(x)	93.8	71.1

Table 1: The top three activation functions discovered by each search strategy, along with the baseline activation functions ReLU and Swish. The functions achieved the highest validation set accuracy after 50 epochs of training with WRN-28-10 on CIFAR-10. The final test accuracies listed on the right are the median of five runs after training WRN-28-10 from scratch for 200 epochs with each activation function on CIFAR-10 and CIFAR-100. Function plots have domain $x \in (-5, 5)$ but have different ranges. Functions marked with an asterisk (*) occasionally did not train to completion due to asymptotes at $x = -\epsilon$. Exhaustive search finds multiple activation functions in a simple search space (S_1) that consistently outperform ReLU and Swish. Evolution with loss-based fitness was the only technique that was able to discover such activation functions in a more complicated search space (S_2), suggesting that it is the most promising technique for scaling up in the future.

The softmax operation converts the fitness values to a probability distribution, allowing functions to be randomly sampled. From the N activation functions, $2(N - m)$ are selected with replacement for reproduction with probability proportional to their fitness. Crossover followed by mutation is applied to the selected activation functions to obtain a new population of size $N - m$. In order to increase exploration, m randomly generated functions are added to a population that will again be of size N . This process is repeated for several generations, and the activation functions with the best performance over the history of the search are returned as a result.

4 EXPERIMENTS AND SETUP

This section presents experiments with multiple architectures, datasets, and search strategies.

4.1 Architectures and Datasets

A wide residual network [22] with depth 28 and widening factor 10 (WRN-28-10), implemented in TensorFlow [1], is trained on

the CIFAR-10 and CIFAR-100 image datasets [10]. The architecture is comprised of repeated residual blocks which apply batch normalization and ReLU prior to each convolution. In the experiments, all ReLU activations are replaced with a candidate activation function. No other changes to the architecture are made. Hyperparameters are chosen to mirror those of Zagoruyko and Komodakis [22] as closely as possible. Featurewise center, horizontal flip, and ZCA whitening preprocessing are applied to the datasets. Dropout probability is 0.3, and the architecture is optimized using stochastic gradient descent with Nesterov momentum 0.9. WRN-40-4 (a deeper and thinner wide residual network architecture) is also used in some experiments for comparison.

The CIFAR-10 and CIFAR-100 datasets both have 50K training images, 10K testing images, and no standard validation set. To prevent overfitting, balanced validation splits are created for both datasets by randomly selecting 500 images per class from the CIFAR-10 training set and 50 images per class from the CIFAR-100 training set. The test set is not modified so that the results can be compared with other work.

Activation Function	Mean Accuracy (95% C.I.)	Repeats
Best from S_1	74.2 (± 0.1)	50
Best from S_2	74.0 (± 0.2)	15
ReLU	73.2 (± 0.2)	50
Swish	49.6 (± 11.6)	25

Activation Functions	t -statistic; p -value
Best from S_1 vs. ReLU	9.73; 4.64×10^{-16}
Best from S_1 vs. Swish	5.91; 9.91×10^{-8}
Best from S_2 vs. ReLU	4.51; 2.91×10^{-5}
Best from S_2 vs. Swish	3.17; 2.98×10^{-3}

Table 2: Confidence intervals (95%) and independent t -tests comparing mean accuracies after training WRN-28-10 on CIFAR-100 for 200 epochs with the best function from S_1 , $(\arctan(x)) * (\min\{x, 0\})$, the best function from S_2 , $(-(\arctan((x^3))) * (\cos(1)))) * (-(\arctan(\min\{x, 0\})) * (\max\{|x|, 0\}))$, and baseline functions ReLU and Swish. The discovered functions perform significantly better than both baselines. WRN-28-10 was not trained 50 times with Best from S_2 and with Swish due to time constraints. In repeated trials, Swish occasionally caused the network to stall during training, explaining its low mean accuracy.

To discover activation functions, a number of search strategies are used. Regardless of the strategy, the training set always consists of 45K images while the validation set contains 5K images; the test set is never used during the search. All ReLU activations in WRN-28-10 are replaced with a candidate activation function and the architecture is trained for 50 epochs. The initial learning rate is set to 0.1, and decreases by a factor of 0.2 after epochs 25, 40, and 45. Training for only 50 epochs makes it possible to evaluate many activation functions without excessive computational cost.

The top three activation functions by validation accuracy from the entire search are returned as a result. For each of these functions, a WRN-28-10 is trained from scratch for 200 epochs. The initial learning rate is set to 0.1, and decreases by a factor of 0.2 after epochs 60, 120, and 160, mirroring the work by Zagoruyko and Komodakis [22]. After training is complete, the test set accuracy is measured. The median test accuracy of five runs is reported as the final result, as is commonly done in similar work in the literature [16].

4.2 Search Strategies

Three different techniques are used to explore the space of activation functions: exhaustive search, random search, and evolution. Exhaustive search evaluates every function in S_1 , while random search and evolution explore S_2 . It is noteworthy that evolution is able to discover high-performing activation functions in S_2 , where the search space contains over 41 billion possible function strings.

4.2.1 Exhaustive Search. Ramachandran et al. search for activation functions using reinforcement learning and argue that simple activation functions consistently outperform more complicated ones [16]. Although evolution is capable of discovering high-performing, complex activation functions in an enormous search space, exhaustive search can be effective in smaller search spaces. S_1 , for example, contains 3,456 possible function strings.

4.2.2 Random Search. An illustrative baseline comparison with evolution is random search. Instead of evolving a population of 50 activation functions for 10 generations, 500 random activation functions from S_2 are grouped into 10 “generations” of 50 functions each.

4.2.3 Evolution. As shown in Figure 3, evolution discovers better activation functions more quickly than random search in S_2 , a search space where exhaustive search is infeasible. During evolution, candidate activation functions are assigned a fitness value based on either accuracy or loss on the validation set. Accuracy-based fitness favors exploration over exploitation: activation functions with poor validation accuracy still have a reasonable probability of surviving to the next generation. A hypothetical activation function that achieves 90% validation accuracy is only 2.2 times more likely to be chosen for the next generation than a function with only 10% validation accuracy since $e^{0.9}/e^{0.1} \approx 2.2$.

Loss-based fitness sharply penalizes poor activation functions. It finds high-performing activation functions more quickly, and gives them greater influence over future generations. An activation function with 0.01 validation loss is 21,807 times more likely to be selected for the following generation than a function with a validation loss of 10. $e^{-0.01}/e^{-10} \approx 21807$.

Both experiments begin with an initial population of 50 random activation functions ($N = 50$), and run through 10 generations of evolution. Each new generation of 50 activation functions is comprised of the top five functions from the previous generation, 10 random functions ($m = 10$), and 35 functions created by applying crossover and mutation to existing functions in the population, as described in Section 3. Ten generations of evolution takes approximately 2,000 GPU hours using GeForce GTX 1080 GPUs.

4.3 Activation Function Specialization

An important question is the extent to which activation functions are specialized for the architecture and dataset for which they were evolved, or perform well across different architectures and datasets. To address this question, activation functions discovered for WRN-28-10 on CIFAR-10 are transferred to WRN-40-4 on CIFAR-100. These activation functions are compared with the best from a small search (1.9K activation functions from S_1) with WRN-40-4 on CIFAR-100.

5 RESULTS

This section presents the experimental results, which demonstrate that evolved activation functions can outperform baseline functions like ReLU and Swish.

Activation Function	Accuracy
$\sigma(x) * \text{erf}(x)$	72.6
$\tanh(x) * \min\{x, 0\}$	72.1
Swish(x)	71.1
ReLU(x)	71.0

Table 3: Test set accuracy of WRN-40-4 with various activation functions after 200 epochs of training on CIFAR-100. Results reported are median of five runs. The top activation function discovered for WRN-28-10 on CIFAR-10, $\tanh(x) * \min\{x, 0\}$, successfully transfers to this new task, outperforming both baselines. However, a search designed specifically for WRN-40-4 on CIFAR-100 discovers a novel activation function, $\sigma(x) * \text{erf}(x)$ that results in even higher performance. This result demonstrates that the main power of activation function metalearning is to be able to specialize the function to the architecture and dataset.

5.1 Improving Performance

Table 1 lists the activation functions that achieved the highest validation set accuracies after 50 epochs of training with WRN-28-10 on CIFAR-10. The top three activation functions for each search strategy are included. To emulate their true performance, a WRN-28-10 with each activation function was trained for 200 epochs five times on both CIFAR-10 and CIFAR-100 and evaluated on the test set. The median accuracy of these tests is reported in Table 1. Although no search was performed on CIFAR-100 with WRN-28-10, the functions that perform well on CIFAR-10 successfully generalize to CIFAR-100.

The best three activation functions discovered through exhaustive search in S_1 outperform ReLU and Swish. This finding shows how important it is to have an effective search method. There are good functions even in S_1 . It is likely that there are even better functions in S_2 , but with billions of possible functions, a more sophisticated search method is necessary.

The activation functions discovered by random search have unintuitive shapes (Table 1). Although they fail to outperform the baseline activation functions, it is impressive that they still consistently reach a reasonable accuracy. One of the functions (marked with *) in Table 1 discovered by random search occasionally failed to train to completion due to an asymptote at $x = -\epsilon$.

Evolution with accuracy-based fitness is less effective because it does not penalize poor activation functions severely enough. One of the functions failed to learn anything better than random guessing. It was likely too sensitive to random initialization or was unable to learn with the slightly different learning rate schedule of a full 200-epoch training. Another function (marked with *) in Table 1 often did not train to completion due to an asymptote at $x = -\epsilon$. The one function that consistently trained well still failed to outperform ReLU.

Evolution with loss-based fitness is able to find good functions in S_2 . One of the three activation functions discovered by evolution outperformed both ReLU and Swish on CIFAR-10, and two of the three discovered outperformed ReLU and Swish on CIFAR-100. Figure 4 shows the top activation function after each generation

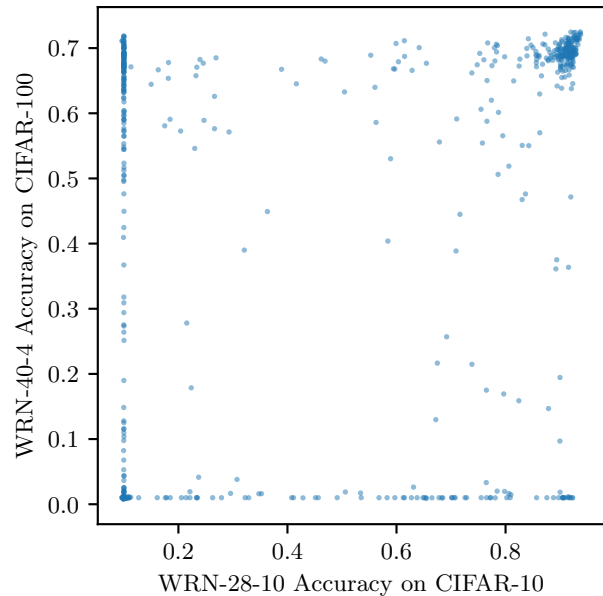


Figure 5: Activation function accuracy across tasks. Each data point represents validation accuracy when training with a given activation function from S_1 with WRN-40-4 on CIFAR-100 for 50 epochs, and with WRN-28-10 on CIFAR-10 for 50 epochs. Some activation functions perform well when paired with a different architecture and dataset. Other functions are specialized to a given architecture and dataset, and do not transfer. The results suggest that reasonable performance can be expected from general evolved activation functions, but that the best performance comes from evolving activation functions for a specific task.

of loss-based evolution. This approach discovered both novel and unintuitive functions that perform reasonably well, as well as simple, smooth, and monotonic functions that outperform ReLU and Swish. It is therefore the most promising search method in large spaces of activation functions.

The performance gains on CIFAR-10 are consistent but small, and the improvement on CIFAR-100 is larger. It is possible that more difficult datasets provide more room for improvement that a novel activation function can exploit.

To evaluate the significance of these results, WRN-28-10 was trained on CIFAR-100 for 200 epochs 50 times with ReLU, 50 times with the best function found by exhaustive search in S_1 , $(\arctan(x)) * (\min\{x, 0\})$, 25 times with Swish, and 15 times with the best function found by evolution in S_2 , $(-(\arctan((x)^3)) * (\cos(1)))) * (-(\arctan(\min\{x, 0\})) * (\max\{|x|, 0\})))$. Table 2 shows 95% confidence intervals and the results of independent t -tests comparing the mean accuracies achieved with each activation function. The results show that replacing a baseline activation function with an evolved one results in a statistically significant increase in accuracy.

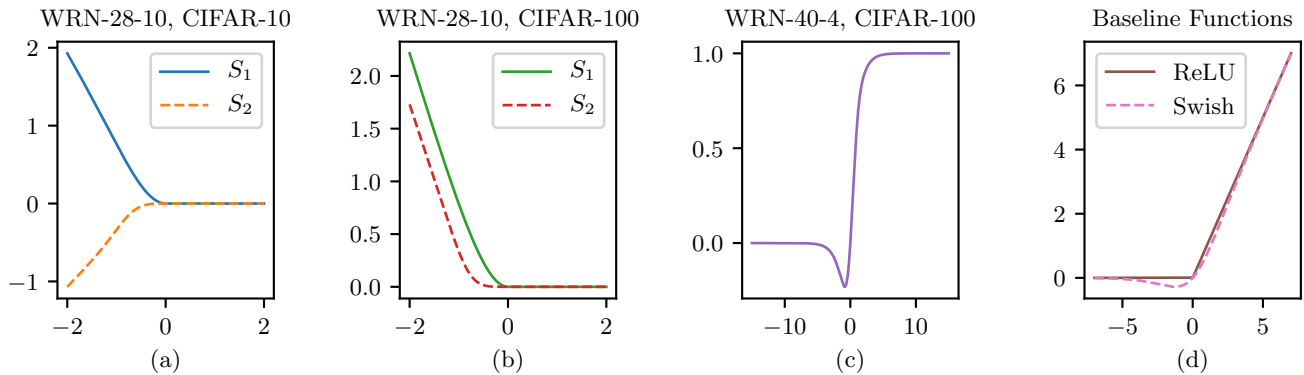


Figure 6: A summary of the best activation functions found in this paper. (a): Exhaustive search in S_1 discovers $(\tanh(x)) * (\min\{x, 0\})$, and evolution in S_2 discovers $(e^{(\min\{\operatorname{erf}(x), 0\}) - (\max\{x, 0\})}) * (\min\{(\arctan((x)^3)) * (\max\{|x|, 0\}), 0\})$. Both functions achieve a median test accuracy of 94.1 with WRN-28-10 on CIFAR-10, outperforming that of ReLU (94.0) and Swish (93.8). (b): The functions $(\arctan(x)) * (\min\{x, 0\})$ in S_1 and $(-((\arctan((x)^3)) * (\cos(1)))) * (-((\arctan(\min\{x, 0\})) * (\max\{|x|, 0\})))$ in S_2 outperform ReLU and Swish by statistically significant margins with WRN-28-10 on CIFAR-100, demonstrating the power of novel activation functions. (c): Functions evolved for WRN-28-10 on CIFAR-10 perform well with WRN-40-4 on CIFAR-100, but a new function discovered specifically for WRN-40-4 on CIFAR-100, $\sigma(x) * \operatorname{erf}(x)$, achieves even higher performance. This result shows that the biggest advantage of activation function metalearning is the ability to discover functions that are specialized to the architecture and dataset. (d): The baseline activation functions, ReLU and Swish, are included for visual comparison.

5.2 Specialized Activation Functions

Since different functions are seen to emerge in different experiments, an important question is: How general or specialized are they to a particular architecture and dataset? To answer this question, the top activation function discovered for WRN-28-10 on CIFAR-10, $\tanh(x) * \min\{x, 0\}$, was trained with WRN-40-4 on CIFAR-100 for 200 epochs. This result was then compared with performance achieved by $\sigma(x) * \operatorname{erf}(x)$, an activation function discovered specifically for WRN-40-4 on CIFAR-100. Table 3 summarizes the result: The activation function discovered for the first task does transfer to the second task, but even higher performance is achieved when a specialized function is discovered specifically for the second task.

The specialized activation function, $\sigma(x) * \operatorname{erf}(x)$, is shown in Figure 6c. It is similar to $\sigma(x)$ in that it tends towards 0 as $x \rightarrow -\infty$, and approaches 1 as $x \rightarrow \infty$. It differs from $\sigma(x)$ in that it has a non-monotonic bump for small, negative values of x . A 50-epoch training of WRN-40-4 on CIFAR-100 with activation $\sigma(x)$ achieved validation accuracy of just 63.2. The superior performance of $\sigma(x) * \operatorname{erf}(x)$ suggests that the negative bump was important, as the shapes of the two activation functions are otherwise similar. This result demonstrates how evolution can discover specializations that make a significant difference.

6 DISCUSSION AND FUTURE WORK

Among the top activation functions discovered, many are smooth and monotonic. Hand-engineered activation functions frequently share these properties [15]. Two notable exceptions were found by random search and evolution with accuracy-based fitness. Although these functions do not outperform ReLU, the fact that WRN-28-10 was able to achieve such high accuracy with these arbitrary

functions raises questions as to what makes an activation function effective. Ramachandran et al. [16] asserted that simpler activation functions consistently outperformed more complicated ones. However, the high accuracy achieved with activation functions discovered by evolution in S_2 demonstrates that complicated activation functions can compete with simpler ones. Such flexibility may be particularly useful in specialization to different architectures and datasets. It is plausible that there exist many unintuitive activation functions which can outperform the more general ones in specialized settings. Evolution is well-positioned to discover them.

Activation functions discovered by evolution perform best on the architectures and datasets for which they were evolved. Figure 5 demonstrates this principle. More generally, it shows the performance of several activation functions when trained with WRN-28-10 for 50 epochs on CIFAR-10 and when trained with WRN-40-4 for 50 epochs on CIFAR-100. Activation functions that perform well for one task often perform well on another task, but not always. Therefore, if possible, one should evolve them specifically for each architecture and dataset. However, as the results in Section 5 show, it is feasible to evolve using smaller architectures and datasets and then transfer to scaled up architectures and more difficult datasets within the same domain.

In the future, it may be possible to push such generalization further, by evaluating functions across multiple architectures and datasets. In this manner, evolution may be able to combine the requirements of multiple tasks, and discover functions that perform well in general. However, the main power in activation function metalearning is to discover functions that are specialized to each architecture and dataset. In that setting most significant improvements are possible.

7 CONCLUSION

Multiple strategies for discovering novel, high-performing activation functions were presented and evaluated: namely exhaustive search in a small search space (S_1) and random search and evolution in a larger search space (S_2). Evolution with loss-based fitness finds activation functions that achieve high accuracy and outperform standard functions such as ReLU and novel functions such as Swish, demonstrating the power of search in large spaces. The best activation functions successfully transfer from CIFAR-10 to CIFAR-100 and from WRN-28-10 to WRN-40-4. However, the main power of activation function metalearning is in finding specialized functions for each architecture and dataset, leading to significant improvement.

ACKNOWLEDGMENTS

This research was supported in part by NSF under grant DBI-0939454 and by DARPA under grant FA8750-18-C-0103. The authors acknowledge the Texas Advanced Computing Center (TACC) at The University of Texas at Austin for providing HPC resources that have contributed to the research results reported within this paper.

REFERENCES

- [1] M. Abadi, P. Barham, J. Chen, Z. Chen, A. Davis, J. Dean, M. Devin, S. Ghemawat, G. Irving, M. Isard, et al. 2016. Tensorflow: A system for large-scale machine learning. In *12th {USENIX} Symposium on Operating Systems Design and Implementation ({OSDI} 16)*. 265–283.
- [2] B. Baker, O. Gupta, N. Naik, and R. Raskar. 2016. Designing neural network architectures using reinforcement learning. *arXiv preprint arXiv:1611.02167* (2016).
- [3] X. Chen, L. Xie, J. Wu, and Q. Tian. 2019. Progressive differentiable architecture search: Bridging the depth gap between search and evaluation. In *Proceedings of the IEEE International Conference on Computer Vision*. 1294–1303.
- [4] T. Elsken, J. H. Metzen, and F. Hutter. 2019. Neural Architecture Search: A Survey. *Journal of Machine Learning Research* 20, 55 (2019), 1–21.
- [5] M. Feurer, J. T. Springenberg, and F. Hutter. 2015. Initializing bayesian hyperparameter optimization via meta-learning. In *Twenty-Ninth AAAI Conference on Artificial Intelligence*.
- [6] C. Finn, P. Abbeel, and S. Levine. 2017. Model-agnostic meta-learning for fast adaptation of deep networks. In *Proceedings of the 34th International Conference on Machine Learning-Volume 70*. JMLR. org, 1126–1135.
- [7] C. Finn and S. Levine. 2017. Meta-learning and universality: Deep representations and gradient descent can approximate any learning algorithm. *arXiv preprint arXiv:1710.11622* (2017).
- [8] S. Gonzalez and R. Miikkulainen. 2019. Improved Training Speed, Accuracy, and Data Utilization Through Loss Function Optimization. *arXiv preprint arXiv:1905.11528* (2019).
- [9] A. Hagg, M. Mensing, and A. Asteroth. 2017. Evolving parsimonious networks by mixing activation functions. In *Proceedings of the Genetic and Evolutionary Computation Conference*. 425–432.
- [10] A. Krizhevsky, G. Hinton, et al. 2009. Learning multiple layers of features from tiny images. (2009).
- [11] A. L. Maas, A. Y. Hannun, and A. Y. Ng. 2013. Rectifier nonlinearities improve neural network acoustic models. In *Proc. icml*, Vol. 30. 3.
- [12] A. Marchisio, M. Hanif, S. Rehman, M. Martina, and M. Shafique. 2018. A Methodology for Automatic Selection of Activation Functions to Design Hybrid Deep Neural Networks. *arXiv preprint arXiv:1811.03980* (2018).
- [13] V. Nair and G. E. Hinton. 2010. Rectified linear units improve restricted boltzmann machines. In *Proceedings of the 27th international conference on machine learning (ICML-10)*. 807–814.
- [14] R. Negrinho and G. Gordon. 2017. Deeparchitect: Automatically designing and training deep architectures. *arXiv preprint arXiv:1704.08792* (2017).
- [15] C. Nwankpa, W. Ijomah, A. Gachagan, and S. Marshall. 2018. Activation functions: Comparison of trends in practice and research for deep learning. *arXiv preprint arXiv:1811.03378* (2018).
- [16] P. Ramachandran, B. Zoph, and Q. V. Le. 2017. Searching for activation functions. *arXiv preprint arXiv:1710.05941* (2017).
- [17] E. Real, A. Aggarwal, Y. Huang, and Q. V. Le. 2019. Regularized evolution for image classifier architecture search. In *Proceedings of the AAAI Conference on Artificial Intelligence*, Vol. 33. 4780–4789.
- [18] E. Real, S. Moore, A. Selle, S. Saxena, Y. L. Suematsu, J. Tan, Q. V. Le, and A. Kurakin. 2017. Large-scale evolution of image classifiers. In *Proceedings of the 34th International Conference on Machine Learning-Volume 70*. JMLR. org, 2902–2911.
- [19] K. Stanley and R. Miikkulainen. 2002. Evolving neural networks through augmenting topologies. *Evolutionary computation* 10, 2 (2002), 99–127.
- [20] M. Wistuba, A. Rawat, and T. Pedapati. 2019. A Survey on Neural Architecture Search. *arXiv preprint arXiv:1905.01392* (2019).
- [21] L. Xie and A. Yuille. 2017. Genetic cnn. In *Proceedings of the IEEE International Conference on Computer Vision*. 1379–1388.
- [22] S. Zagoruyko and N. Komodakis. 2016. Wide residual networks. *arXiv preprint arXiv:1605.07146* (2016).
- [23] B. Zoph and Q. V. Le. 2016. Neural architecture search with reinforcement learning. *arXiv preprint arXiv:1611.01578* (2016).